Article

Applied Spectroscopy

Applied Spectroscopy
0(0) 1–12

DOI: 10.1177/0003702816660725
asp.sagepub.com
SAGE

On the Identification of Rayon/Viscose as a Major Fraction of Microplastics in the Marine Environment: Discrimination between Natural and Man-made Cellulosic Fibers by Fourier Transform Infrared Spectroscopy

Ionela Raluca Comnea-Stancu[1,2], Karin Wieland[1], Georg Ramer[1], Andreas Schwaighofer[1], and Bernhard Lendl[1]

Abstract

This work was sparked by the reported identification of man-made cellulosic fibers (rayon/viscose) in the marine environment as a major fraction of plastic litter by Fourier transform infrared (FT-IR) transmission spectroscopy and library search. To assess the plausibility of such findings, both natural and man-made fibers were examined using FT-IR spectroscopy. Spectra acquired by transmission microscopy, attenuated total reflection (ATR) microscopy, and ATR spectroscopy were compared. Library search was employed and results show significant differences in the identification rate depending on the acquisition method of the spectra. Careful selection of search parameters and the choice of spectra acquisition method were found to be essential for optimization of the library search results. When using transmission spectra of fibers and ATR libraries it was not possible to differentiate between man-made and natural fibers. Successful differentiation of natural and man-made cellulosic fibers has been achieved for FT-IR spectra acquired by ATR microscopy and ATR spectroscopy, and application of ATR libraries. As an alternative, chemometric methods such as unsupervised hierarchical cluster analysis, principal component analysis, and partial least squares-discriminant analysis were employed to facilitate identification based on intrinsic relationships of sample spectra and successful discrimination of the fiber type could be achieved. Differences in the ATR spectra depending on the internal reflection element (Ge versus diamond) were observed as expected; however, these did not impair correct classification by chemometric analysis. Moreover, the effects of different levels of humidity on the IR spectra of natural and man-made fibers were investigated, too. It has been found that drying and re-humidification leads to intensity changes of absorption bands of the carbohydrate backbone, but does not impair the identification of the fiber type by library search or cluster analysis.

Keywords

Man-made cellulose fibers, viscose fibers, natural fibers, rayon, Fourier transform infrared spectroscopy, attenuated total reflection, microscopy, hierarchical cluster analysis, principal component analysis

Date received: 7 June 2016; accepted: 21 June 2016

Introduction

The accumulation of plastic litter and its debris in the environment has recently received a lot of attention, both within the concerned public as well as within the scientific community. When dealing with the problem of plastic litter and its degradation products on a scientific basis, analysis protocols that are "fit for purpose" are required. In general, these protocols must deal with separation of plastic particles from the sample matrix (sediments, sea water, surface

[1]Institute of Chemical Technologies and Analytics, Vienna University of Technology, Vienna, Austria
[2]Faculty of Applied Chemistry and Materials Science, Politehnica University of Bucharest, Bucharest, Romania

Corresponding author:
Bernhard Lendl, Institute of Chemical Technologies and Analytics, Vienna University of Technology, Getreidemarkt 9/164-UPA, 1060 Vienna, Austria.
Email: bernhard.lendl@tuwien.ac.at

water, and alike) as well as they need to ensure that no post-sampling contaminations take place during analysis. Finally, analytical methods need to be applied, which are capable of unambiguous identification of the encountered plastic material. Unfortunately, it appears that the overall difficulty in correct analysis of microplastic materials (fibers, films, fragments, or granular particles smaller than 5 mm) is often underestimated. As a consequence, questionable results are reported which may lead to premature conclusions. Examples concern presumed identification of synthetic particles as contaminants in honey and German beers.[1,2] In a detailed study it appeared most likely that these findings were not correct.[3] Instead of being contamination in honey and German beer, the found and "identified" plastic particles were more likely originating from post-sampling contaminations in the laboratory and application of not fully selective analysis methods (chemical staining). Meanwhile, the problem of post-sampling contamination has been recognized and is frequently discussed.[3,4]

One of the first reports on microplastics in marine environments was published in 2011 and raised the attention for this issue.[5] The authors used Fourier transform infrared (FT-IR) spectroscopy and spectral database matching for identifying the materials. In particular when dealing with the identification of microfibers in the marine or freshwater environment, it is proposed to use a forensic science approach to minimize the risk of contamination.[4] In their paper, Woodall et al. stress the need for a series of measures aimed to avoid contaminations due to the ubiquity of microfibers in the environment.[4] Clothing made from man-made fibers such as acrylic, viscose/rayon, polyester and nylon are common and regarded a potential source of contamination. To avoid this contamination risk, the scientists of this study wore 100% natural fiber clothing, and were covered by a clean 100% white cotton boiler suit, lab coat and headscarf. Furthermore, laboratory work was carried out in a dedicated clean laboratory. Even though strictest measures have been applied, still some cellulosic fibers were found in the samples drawn from the clean room.

Cellulosic fibers were also reported as an important share of microfibers in deep-sea sediment samples in this study. Interestingly, already in 2013, Lusher et al. reported the identification of rayon / viscose fibers in the gastrointestinal tract of fish,[6] and in 2014, Woodall et al. came to the conclusion that rayon fibers are a major source of microplastic debris even in the deep sea.[7] In that particular work, microplastic content of sediments from the deep sea was identified by FT-IR spectroscopy. As claimed by the authors, the obtained results showed evidence for fibers as a large and hitherto unknown repository of microplastics, which supposedly had been underreported in previous studies. Microplastic identification was based on FT-IR transmission measurements using a diamond compression cell (Specac DC2 Diamond compression cell) and fiber identification was performed by library search.[7] Unfortunately, the authors neither provide IR spectra nor details on the performed data analysis, apart from the fact that matches with a quality index of greater than 0.7 were accepted. Furthermore, no efforts to achieve discrimination between natural and man-made cellulosic fibers within the microplastic debris have been described. Nevertheless, the reported conclusions have been taken for granted and found their way also to the general public as seen, for example, from a recent entry in Wikipedia.[8]

The motivation for the present work is based on this situation and targets the question whether an unambiguous identification of man-made cellulosic fibers can be performed. Cellulose fibers are subdivided into natural and man-made fibers. Natural fibers originating from plants are grouped into seed (e.g., cotton), bast (e.g., flax, hemp, kenaf, ramie), leaf (e.g., sisal) as well as tree fibers (e.g. wood).[9,10] These fiber types, except for the tree fibers from wood, have been extensively used for clothing, domestic woven fabrics and ropes for thousands of years. Due to their wide availability, low cost, good recyclability, low density and high-specific mechanical strength, over the last years there has been an increased interest for application as reinforcements in polymer matrix composites, e.g., in the automotive and construction industries.[11]

For production of cellulose based man-made fibers, wood pulp is the most important resource. Derivative and direct methods are used for processing of the pulp to manufacture man-made fibers.[12] In the viscose process, derivatization of cellulose with carbon disulfide is followed by a ripening period and subsequent regeneration of the viscose fiber. Variants of that fiber type include high tenacity rayon (e.g., tire cord) and high wet modulus viscose (e.g., Modal). In Europe, fibers and fabrics produced from regenerated cellulose became known as "viscose," whereas in the U.S. they are termed rayon. In the more recently developed Lyocell process, wood pulp is directly dissolved in an organic solvent (*N*-methylmorpholine *N*-oxide) without prior derivatization. Cellulose fibers obtained by this method are referred to as the generic fiber type Lyocell. Lyocell fibers from Lenzing AG, Austria, are branded as Tencel®. Man-made cellulose fibers are widely used for clothing, interior textiles and hygiene products but can also be manufactured with modified properties for industrial use.[13]

The increasing variety of fiber types and composites as well as a growing interest for industry applications advanced the development of appropriate analytical approaches. Conventional methods including microscopy and staining techniques have limitations as they heavily rely on experience and the fiber morphology is often concealed or destroyed by biological degradation or physical damage.[14] Spectroscopic techniques such as terahertz time domain (THz-TD), Raman, and FT-IR spectroscopy have been used for separate characterization of cellulosic natural and man-made fibers.[14–20]

There is a distinct difference between native and regenerated cellulose regarding their crystal structure. Native cellulose occurring in natural fibers results in a crystal structure referred to as cellulose I. Upon derivatization or dissolution and subsequent regeneration of the viscose fiber, cellulose adopts the crystal structure of cellulose II, which has a modified orientation of the cellulose chains and hydrogen-bonding system.[21] For determination of crystallinity, methods based on wide angle X-ray scattering (WAXS) and nuclear magnetic resonance (NMR) have been introduced.[22–24] A method for the identification of the fiber type based on crystallinity employing FT-Raman and FT-IR spectroscopy has been proposed,[25] however with the drawback of relying on WAXS calibration.

Fourier transform infrared spectroscopy is known as a versatile, nondestructive, and label-free technique for chemical analysis of a wide range of analytes. It offers attractive features such as high sampling rate, fast sample preparation, sound sensitivity, and the capacity for comprehensive qualitative as well as accurate quantitative analysis. This spectroscopic technique has been successfully applied for the analysis of natural and viscose-type fibers.[14,15,18]

Hierarchical cluster analysis (HCA) is a chemometric method to organize a set of objects, characterized by the values of a set of variables, into groups.[26] The combination of spectroscopy and multivariate methods of data analysis allows the investigation of intrinsic relationships of samples according to their spectral similarities. It has been successfully applied in combination with FT-IR spectroscopy for diverse types of samples.[27–29] Partial least squares-discriminate analysis (PLS-DA) has found application in classification and statistical discrimination, especially when the within group variation is greater than that of the between group variation.[30] It is thus a preferred alternative to classification by principal component analysis (PCA).

The scope of this work is to draw attention to possible pitfalls that may occur when aiming at the seemingly trivial task of differentiation between man-made and natural fibers using FT-IR spectroscopy and library search. A comprehensive analysis for identification of different types of natural and man-made cellulosic fibers employing single-reflection attenuated total reflection (ATR) spectroscopy, transmission microscopy, and ATR microscopy is presented. Based on this investigation, a fast and reliable working routine for discrimination of fiber samples into these two groups of fibers is introduced employing library search, HCA, and PLS-DA. Results of different spectrum acquisition methods and evaluation parameters are presented.

Materials and Methods

Samples

For FT-IR analysis, a total of 18 cellulose samples were provided by Lenzing AG, comprising nine different kinds of natural and man-made fibers, respectively. The man-made fibers included several types of viscose fibers as well as Modal and Lyocell fibers. Natural fiber samples contained different sorts of cotton, pulp, ramie, kenaf, hemp, flax and sisal fibers. The samples are summarized in Table 1. Spectra acquisition of fiber samples was performed on single fibers at room temperature, without any prior preparative treatment.

Table 1. Fiber samples for FT-IR analysis.

#	Natural	Man-made
1	raw cotton	viscose #1
2	wood pulp Pöls Orion	viscose #2
3	wood pulp Rosenthal Kraft	viscose #3, with TiO_2
4	ramie	Modal #1
5	cotton, bleached	Modal #2
6	kenaf	Tencel® #1
7	hemp	Tencel® #2
8	flax	tire cord Super 2
9	sisal	tire cord RT 610

FT-IR: Fourier transform infrared.

Experimental Methods

Fourier transform infrared spectra of natural and man-made fiber samples have been recorded using three different spectra acquisition techniques: (1) single-reflection ATR spectroscopy, (2) transmission microscopy and (3) ATR microscopy. Single-reflection ATR FT-IR measurements were performed using a Bruker Tensor 37 spectrometer (Bruker, Ettlingen, Germany) equipped with a DLaTGS (deuterated L-alanine doped triglycine sulfate) detector operated at room temperature using a Bruker Optics Platinum ATR module (diamond crystal, 1 mm^2 area with single reflection). Fourier transform infrared microscopy measurements were performed with a Hyperion 3000 microscope (Bruker, Ettlingen, Germany) equipped with a liquid nitrogen cooled HgCdTe (mercury cadmium telluride, MCT) detector. For transmission microscopy measurements, a Nikon 15 × objective and a "Diamond EX'Press II" compression cell with an aperture of 1.6 mm (S.T. Japan., Cologne, Germany) were used. Attenuated total reflection microscopy spectra were acquired using a Ge-ATR 20× objective. For all measurements, spectra were recorded as the co-addition of 32 scans with a spectral resolution of 4 cm^{-1}. Instrument control and spectrum acquisition were performed with OPUS 7.2 software (Bruker, Ettlingen, Germany). Simulated spectra were computed using antisymmetric linear combinations of Lorentzian functions in MATLAB R2014b (MathWorks, Inc., Natick, MA, 2014).[31]

Library Search

Infrared spectra of natural and man-made fibers were compared with Bruker's "Natural Fibers" and "Synthetic Fibers ATR" IR spectral libraries. The IR library spectra have been acquired by the Bruker HELIOS ATR microsampling accessory. No secured information could be obtained from Bruker Optics which IRE element had been used for recording the spectra in these libraries. Library search was performed employing the spectrum correlation search algorithm using vector normalization of the second-derivative spectra as data pretreatment. For comparison, the library search has been performed using both the entire spectral range (4000–800 cm^{-1}) as well as reduced spectral range (2200–800 cm^{-1}).

Chemometric Analysis Methods

Unsupervised HCA was performed using OPUS 7.2 (Bruker, Germany). Dendrograms were obtained with the Ward's method on the basis of Euclidean distances. Principal component analysis and PLS-DA were performed employing DataLab.[32] Prior to the analysis, second-derivative spectra were vector-normalized and Savitzky–Golay smoothed with five smoothing points. The spectral range for analysis was limited to 1600–800 cm^{-1}.

Results and Discussion

IR Spectroscopy of Fiber Samples

For comparison of spectra acquisition methods, IR spectra of natural and man-made fiber samples have been acquired employing single-reflection ATR spectroscopy, transmission microscopy, and ATR microscopy. The ATR technique allows simple, reproducible, and non-destructive collection of IR spectra and needs hardly any sample preparation.[33] For the single-reflection ATR accessory, the area of interaction is approx. 1 mm^2, while for IR microscopy measurements with the ATR objective, a sample area of approx. $32 \times 32\ \mu m^2$ is analyzed.

Transmission spectra provide information about the bulk composition of the fiber, while ATR spectroscopy is a surface sensitive technique. The penetration depth of IR light into the sample decreases at higher wavenumbers, leading to lower absorbance values in these spectral regions compared to transmission measurements. Using ATR spectroscopy, the penetration depth (d_p) results from the relationship

$$d_p = \frac{\lambda}{2\,\pi\, n_{IRE}\sqrt{sin^2\theta - (n_{Sample}/n_{IRE})^2}} \qquad (1)$$

where λ is the IR wavelength, n_{IRE} the refractive index of the internal reflection element (IRE), n_{sample} the refractive index of the sample, and θ the angle of incidence of the IR beam.[31,33] Given $n_{IRE} = 2.4$ for diamond, $n_{sample} = 1.5$ for the fiber samples, and $\theta = 45°$, the penetration depth into the fibers is 0.3 μm at 4000 cm^{-1} and 1.5 μm at 800 cm^{-1}. In addition to this $1/\nu$ dependence, the penetration depth of IR light also depends on the real part of the refractive indices of the sample and ATR element material, as outlined in Eq. 1. The real part of the refractive index is not constant as it slowly increases with increasing wavenumber (normal dispersion). In wavenumber regions close to an absorption band (i.e., near a peak in the imaginary refractive index) the real part of the refractive index changes across the absorption band with a minimum at the high wavenumber side and a maximum at the low wavenumber side of the absorption band (anomalous dispersion). When comparing ATR spectra with transmission spectra, this accounts for an increase in the penetration depth on the low wavenumber side (due to high real part of the refractive index of the sample) leading to a perceived higher absorption. On the high wavenumber side of the band, anomalous dispersion results in a decrease of the penetration depth and a perceived lower absorption.[33]

Figure 1 shows a comparison of IR spectra recorded with the three acquisition methods on the example of the ramie natural fiber sample. The spectra show characteristic absorption bands in the fingerprint region (1500–800 cm^{-1}), as well as in the spectral regions of 2950–2750 cm^{-1} and 3600–3000 cm^{-1}, attributed to aliphatic C–H stretching vibrations and O–H stretching vibrations, respectively. Infrared spectra acquired with the ATR technique display similar overall appearance and show distinct differences to the IR spectrum acquired by transmission

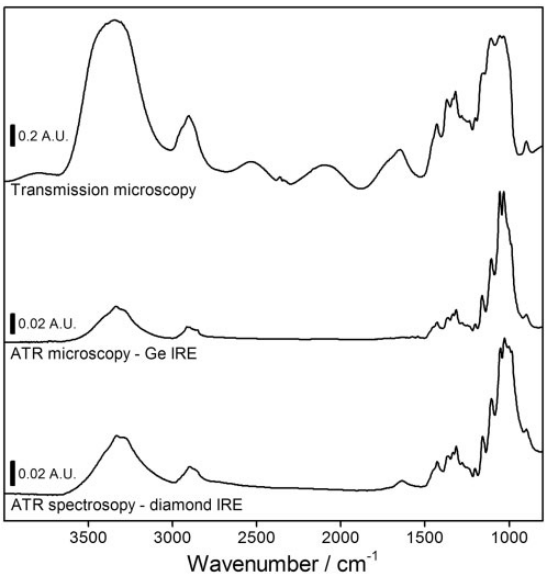

Figure 1. FT-IR absorbance spectra of ramie fiber acquired by transmission microscopy, ATR microscopy, and ATR spectroscopy.

microscopy. Between ATR spectra the absorbance values may vary considerably depending on the force that is applied to press the sample material on the IRE. The differing extent of absorbance particularly in the C–H and O–H stretching region between transmission and ATR spectra can be explained by multiple reasons. Within this context, a fundamental difference between ATR and transmission spectra is that the first represents a surface sensitive technique whereas the latter gathers information about the entire sample cross-section. Following from that there is the possible effect of detector non-linearity on strong bands in transmission spectra measured with an MCT detector.[31]

In the transmission spectrum, sinusoidal modulations of the baseline called interference fringes are observable. These artifacts result from multi-reflections of the IR beam between the plane-parallel windows of the transmission cell. Fringes can hardly be avoided and inevitably lead to distortions in the IR spectrum, impeding the qualitative and quantitative interpretation of the spectra. A further challenge involving the sample preparation of solid samples for IR transmission microscopy is the adjustment of the sample thickness. In this study, a diamond compression cell has been used to compress the fiber samples from their native diameter (10–25 μm) to a thickness that is applicable for transmission spectroscopy. The sample thickness was adjusted so that the absorbance of the strongest bands was less than 1.5 A.U. The detector response was found to be linear because the peak absorbance of the strong bands did not change when a 50% transmitting screen was inserted into the beam.

With regard to the present fiber samples, the discussed differences between transmission and ATR spectra may lead to different appearance of the spectra due to the diverging composition and structure of the fiber core and surface. Particularly in natural fibers, the chemical composition of the fiber surface varies from the core,[34] which may not be accessible by the ATR technique when considering the thickness of fibers ranging from 10 to 25 μm.[35]

Figure 2 shows representative ATR FT-IR spectra of three natural and three man-made fiber samples. Table 2 presents the most significant absorption bands and their assignments based on previous references.[14,15,18,36] Since cellulose is the predominant component for both natural and man-made fibers, the spectra of either group of fiber samples appear similar at first glance. However, there are certain characteristic features that can be assigned to the two groups of fiber samples. One is the characteristic profile of the O–H stretching band. While the shape of this band is rather broad and featureless for man-made fibers, it exhibits a distinct maximum at 3330 cm^{-1} for natural fibers. In addition, the band at 1735 cm^{-1} has not been observed for any man-made fiber samples, but appeared in several natural fiber samples (flax, hemp, sisal), and can be related to their pectin content.[37,38] A strong band in IR spectra of

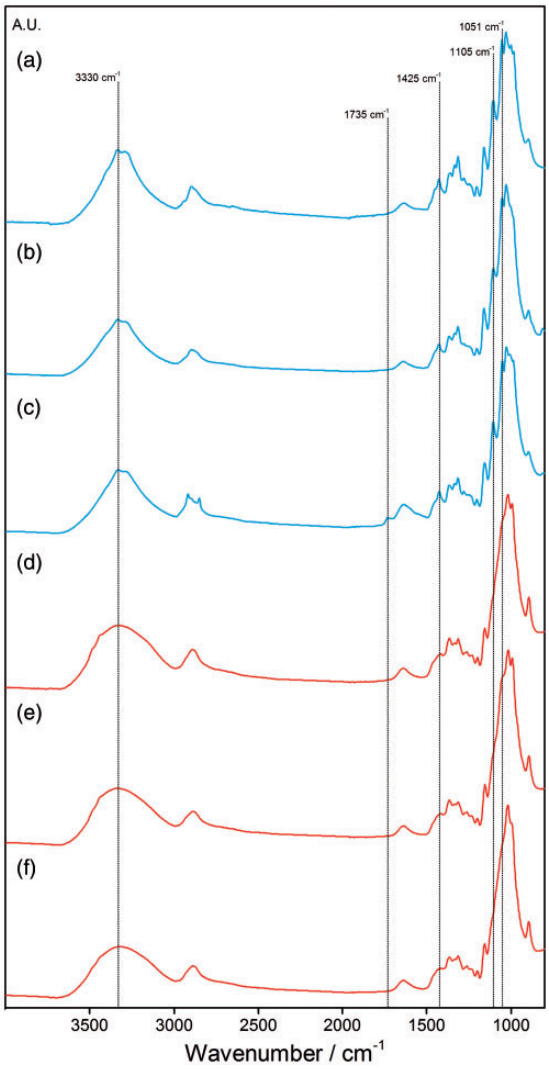

Figure 2. Representative ATR FT-IR absorbance spectra of three natural (a–c, blue) and three man-made fiber samples (d–f, red): (a) raw cotton, (b) wood pulp Rosenthal Kraft, (c) flax, (d) Tencel® #1, (e) Modal #1, (f) viscose #1.

natural fibers at 1425 cm^{-1} assigned to CH_2 or O–C–H bending appears weak and shifted to 1420 cm^{-1} for man-made fibers, which is in accordance with prior reports.[39] Further, absorption bands at 1105 and 1051 cm^{-1} assigned to the antisymmetric and symmetric C–O–C stretching modes, respectively, show high intensity for natural fibers but merely appear as shoulders in man-made fiber samples.

Library Search

As an attempt to establish a routine for the discrimination between natural and man-made fiber samples, comparison of the acquired spectra with a spectral library has been performed. Rather than the specific identification of the kind and origin of the fibers, the aim is to categorize the samples as natural or man-made fibers. For this purpose,

Table 2. Characteristic frequencies of main absorption bands in ATR-FT-IR spectra and band assignments for natural and man-made fibers.[14,15,18,36]

Natural fibers		Man-made fibers		
experimental (cm^{-1})	literature (cm^{-1})	experimental (cm^{-1})	literature (cm^{-1})	Assignment
3330	3600–3100[36]	3487	3488[18]	O–H stretching, intra- and intermolecular H bonds
3289	3600–3100[36]	3445	3447[18]	O–H stretching, intra- and intermolecular H bonds
2897	2900[18]	2892	2900[18]	C–H stretching
1735	1735[14]	–	–	C = O stretching of an ester
1640	1635[14]	1640	1635[14]	HOH bending of absorbed water
1458	1460[36]	–	–	O–H in plane bending
1425	1423[15]	1420	1423[15]	H–C–H, O–C–H in plane bending
1366	1365[14]	1364	1375[18]	Symmetric CH_3 deformation
1335	1335[18]	1335	1335[18]	O–H in plane bending
1317	1317[18]	1313	1315[18]	C–H wagging
1279	1282[18]	1263	1278[18]	C–H bending
1247	1245[15]	–	–	C–C, C–O, C = O stretching
–	–	1230	1232[15]	C–O–H bending
1203	1205[18], 1200[36]	1199	1200[18]	O–H in plane bending
1160	1155[18], 1150[36]	1156	1162[18]	C–O–C antisymmetric stretching
1105	1105[14]	–	–	C–O–C antisymmetric stretching
1051	1055[18], 1050[14]	1057	1055[18], 1050[14]	C–O–C symmetric stretching
1030	1035[18]	1023	1035[18]	C–O stretching

ATR: attenuated total reflection.

the "Natural Fibers" and "Synthetic Fibers ATR" libraries by Bruker have been used. In order to evaluate the effect of different spectral ranges on the results of the library search, the procedure was performed on the one hand using the entire spectral range, and on the other hand using a reduced spectral range (2200–800 cm^{-1}).

Initially, a standard algorithm based on comparison of band parameters in the FT-IR absorbance spectrum was applied. Using this search algorithm, the identification rate of the fiber groups was merely 20–30 % across all spectra acquisition methods. Consequently, the procedure was refined and a spectrum correlation search algorithm was employed using vector normalization of the second-derivative spectra as data pretreatment. Vector normalization suppresses random intensity differences between sample and library spectra and by comparing the second derivatives of the IR spectra, variances in the baseline offset and sloping baselines are eliminated.

Exemplary results of the library search (first three hits) using IR spectra obtained with the three different spectra acquisition methods of a natural and man-made fiber sample are shown in Table 3. The hit quality (HQ) provides information on the congruence between the sample spectrum and the library spectrum based on band position, relative intensity and the full width at half maximum of the band. The HQ value is ranged between 0 and 1000, indicating a lack of congruence and perfect match, respectively. Values for HQ differ considerably between transmission spectra and ATR spectra. In general, the hit quality for transmission spectra is considerably lower than for ATR spectra, with comparable values for ATR microscopy and ATR spectroscopy. An explanation for this tendency may be that the library spectra have been acquired by an ATR microsampling accessory resulting in a higher analogy to ATR sample spectra than to transmission sample spectra. As further discussed below, for ATR measurements, the employed IRE material might impact the results of the library search. Regarding the different spectral ranges used for library search, there is no distinct difference in HQ.

A comprehensive comparison of the identification rate of the fiber type employing the three different spectra acquisition methods is shown in Figure 3. For this evaluation, the three findings with the highest HQ of library searches of duplicate measurements have been considered. The results indicate that the choice of the spectral region used for library search does not substantially change the rate of fiber type identification, provided that the spectral region comprising the most prominent bands (800–1750 cm^{-1}, see Table 2) is included. The lowest identification rate has been found for transmission microscopy. This can be explained by varying spectra quality as a result of

Table 3. Exemplary results of the library search (first three hits) using IR spectra obtained with the three different spectra acquisition methods of a natural (ramie) and man-made (viscose #1) fiber. Red color indicates incorrect identification of fiber group, implying that a natural fiber is identified as a man-made fiber, or vice versa (HQ, hit quality).

	Natural fiber				Man-made fiber			
	Library search reduced spectral range		Library search entire spectral range		Library search reduced spectral range		Library search entire spectral range	
Method of analysis	HQ	Results	HQ	Results	HQ	Results	HQ	Results
Transmission microscopy	376	Linen	365	Viscose rayon, filament	651	Solution dyed rayon	594	Solution dyed rayon
	375	Viscose rayon, filament	363	Linen	415	70/30 Rayon/ Polyester blend	442	70/30 Rayon/ Polyester blend
	365	Lokta tree bark, Nepal	355	Lokta tree bark, Nepal	412	Linen	442	Linen
ATR microscopy	752	India village paper	720	India village paper	719	Industrial yarn, Rayon, 1100/720	714	Industrial yarn, Rayon, 1100/720
	738	Straw paper, India	709	Straw paper, India	716	Rayon tire chord	707	Rayon tire chord
	734	Wool paper, India	704	Wool paper, India	701	Industrial Yarn, Rayon, 2200/1440	697	Industrial yarn, Rayon, 2200/1440
ATR spectroscopy	888	Kozo tree fiber paper, Japan	874	Kozo tree fiber paper, Japan	671	Solution dyed rayon	626	Solution dyed rayon
	883	Straw paper, India	864	Straw paper, India	582	Lokta tree bark, Nepal	551	Industrial yarn, Rayon, 1100/720
	859	Wool paper, India	841	Wool paper, India	579	Industrial yarn, Rayon, 2100/1400	550	Lokta tree bark, Nepal

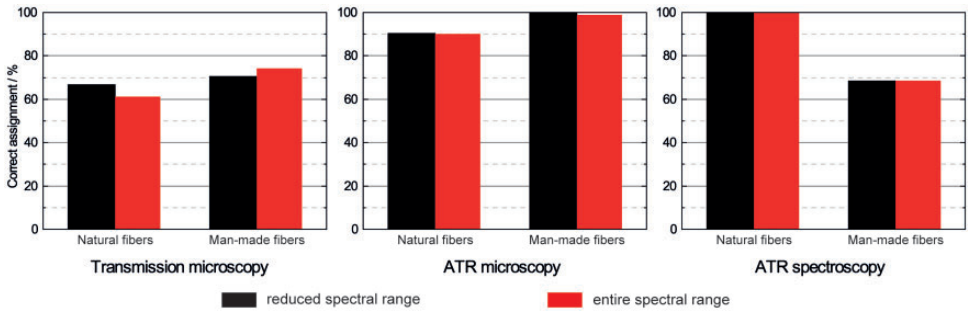

Figure 3. Percentages of correct identification of natural and man-made fibers with transmission microscopy, ATR microscopy and ATR spectroscopy by library search (second derivative, vector normalization), applying the entire spectral range (4000–800 cm^{-1}) and reduced spectral range (2200–800 cm^{-1}).

fringes (see Figure 1), and the difference between spectra acquisition methods of the sample and the library spectra, as aforementioned. Searching the recorded ATR spectra against the library spectra clearly provided a better means to distinguish between the two types of cellulosic fibers. The highest rate of identification has been achieved by ATR microscopy, where over 90 % of hits recognized the correct group of fiber when using the entire spectral range for library search. For ATR spectroscopy, 100% of natural fiber sample have been identified correctly, but only approx. 70 % of man-made fiber samples. Within the two ATR techniques used in this study, no significant difference regarding identification of the fiber type has been obtained (see Figure 3).

The results of this library search suggest that the type of data pretreatment plays a crucial role for the success of fiber categorization, whereas the choice of the spectral range only has minor influence. Further, the rate of fiber type identification can be improved by matching the sample acquisition technique (transmission/ATR) with library spectra. Visual inspection and comparison of sample and library spectra is strongly recommendable in any case.

Cluster Analysis

Unsupervised HCA was performed to evaluate its potential to discriminate between natural and man-made fiber samples based on grouping of IR spectra according to their similarities. Within the present work, the advantage of this multivariate technique is that it compares IR spectra recorded at the same instrument with identical acquisition parameters. For library search using commercial spectra libraries, details about acquisition parameters are often not available. However, for identification of the fiber group of an unknown sample using HCA, reference fibers with known origin are essential.

As for the library search, spectra pretreatment significantly influences the outcome of HCA. Optimum results were obtained for second-derivatized and vector-normalized spectra as well as limiting the spectral range for analysis to 1600–800 cm^{-1}. Using these parameters, grouping of sample spectra into two clusters containing natural and man-made fibers, respectively, could be obtained when using ATR microscopy and ATR spectroscopy. Figure 4 shows dendrograms obtained by HCA of transmission microscopy and ATR microscopy spectra of all studied fiber samples. For the spectra acquired by ATR microscopy (Figure 4(a)), there is a clear formation of two compact clusters with distinct differentiation on the heterogeneity scale containing natural and man-made fibers, respectively. For unknown samples, the fiber type can then be identified by attribution to one of the two groups. For IR spectra recorded by transmission microscopy, however, clustering into two groups could not be observed (Figure 4(b)). Furthermore, upon performing PCA, clustering into two distinct groups could also be obtained for ATR microscopy, but not for transmission microscopy (data not shown).

Influence of the IRE Material on ATR Spectra

As outlined in Eq. 1, the refractive index of the IRE strongly affects the penetration depth as well as anomalous dispersion and consequently the resulting spectra. Assuming the same angle of incidence ($\theta = 45°$), the penetration depth of a germanium IRE ($n_{Ge} = 4.0$) is smaller by a factor of 2.2 than for a diamond IRE.[31] Figure 5 illustrates the effect of anomalous dispersion on an absorption band. At low absorption indices ($k_{max} = 0.01$), the shift of the band maximum towards lower wavenumbers is small for both IRE elements. However, at particularly high absorption indices ($k_{max} = 0.3$), the computed spectra reveal a band shift due to anomalous dispersion as high as 5 cm^{-1} in the case of the diamond IRE. Values for k have been selected as these are characteristic for strong and small absorbing bands of organic substances in this spectral range.[31] For germanium, the band shift is lower due to the higher difference between n_{IRE} and n_{sample}. A comparable shift in region of the C-O stretching bands

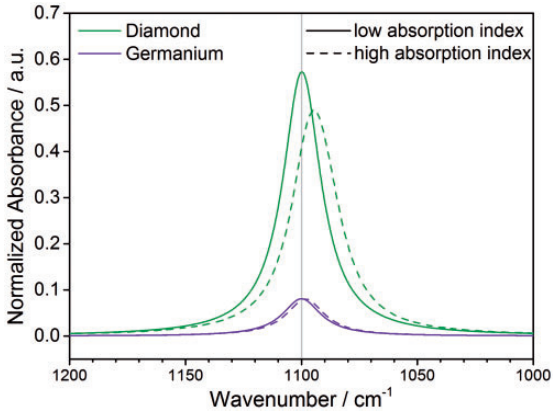

Figure 5. Calculated ATR spectra of an absorption band at 1100 cm^{-1} with (solid) low absorption index ($k_{max} = 0.01$) and (dashed) high absorption index ($k_{max} = 0.3$) for (green) a diamond and (purple) a germanium IRE element. The solid gray line indicates the position of the band maximum in a transmission measurement.

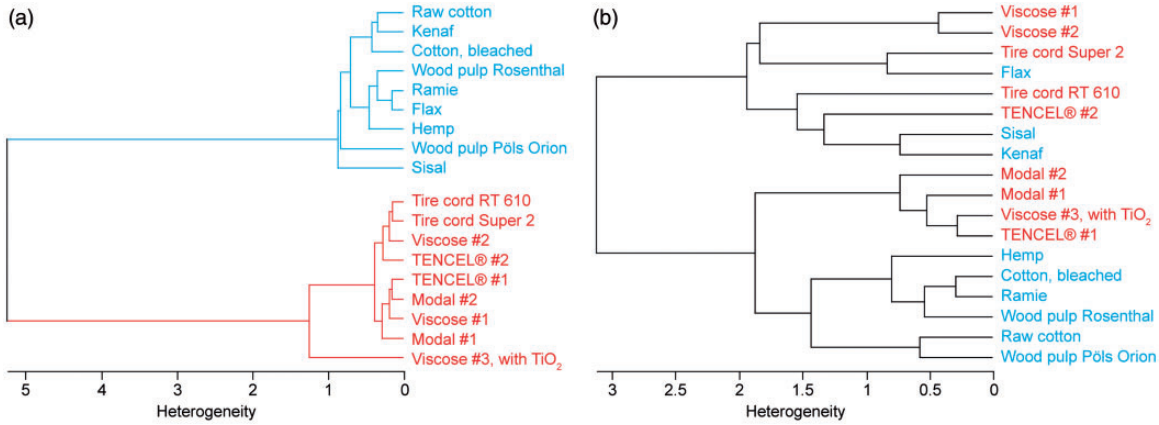

Figure 4. Dendrogram obtained with the Ward's method calculated by Euclidean distances of (a) ATR FT-IR microscopy spectra and (b) transmission microscopy spectra of natural and man-made fiber samples using the optimized HCA parameters.

can be observed in the experimental spectra shown in Figure 1.

Following from that, similar results could be expected for ATR microscopy and standard ATR spectroscopy, if the same IRE is employed. Considering the result obtained from the spectral library search, no clear difference in the capability to differentiate between man-made and natural fibers by ATR spectroscopy and ATR microscopy on basis of the available library spectra could be found. Performing HCA and PCA with all recorded ATR spectra (diamond and germanium) of both fiber types obtained the results depicted in Figure 6. The clustering is influenced by both, the type of the cellulose fiber (man-made vs. natural) as well as the type of IRE (diamond vs. germanium) used for obtaining ATR spectra. However, HCA results reveal that for this particular application the heterogeneity in the spectra introduced by the fiber type was larger than the one introduced by the different IRE material. This outcome is corroborated by PCA, as the largest variation in the data set (PC 1) has been found between natural and man-made fibers.

Finally, for distinguishing between man-made and natural fibers on basis of ATR spectra, a model based on PLS-DA was developed. The calibration model comprising spectra acquired with both IRE elements showed a sensitivity and specificity of 100%. For validation, the obtained data set of natural and man-made fiber spectra has been randomly divided into calibration and validation (4 data points of natural and man-made fibers, respectively) sets. Figure 7 demonstrates the excellent performance of the established PLS-DA model for correct prediction of the fiber type.

Influence of Humidity Changes on the IR Spectra of Natural and Man-Made Fibers

Natural and man-made cellulosic fibers show strong hydrophilic behavior which leads to different levels of water absorption depending on the degree of humidity in the environment. It has been shown that water uptake leads to structural modifications of the fiber.[40] In order to study the effect of water absorption and desorption on natural and man-made fibers, time-dependent IR spectra were

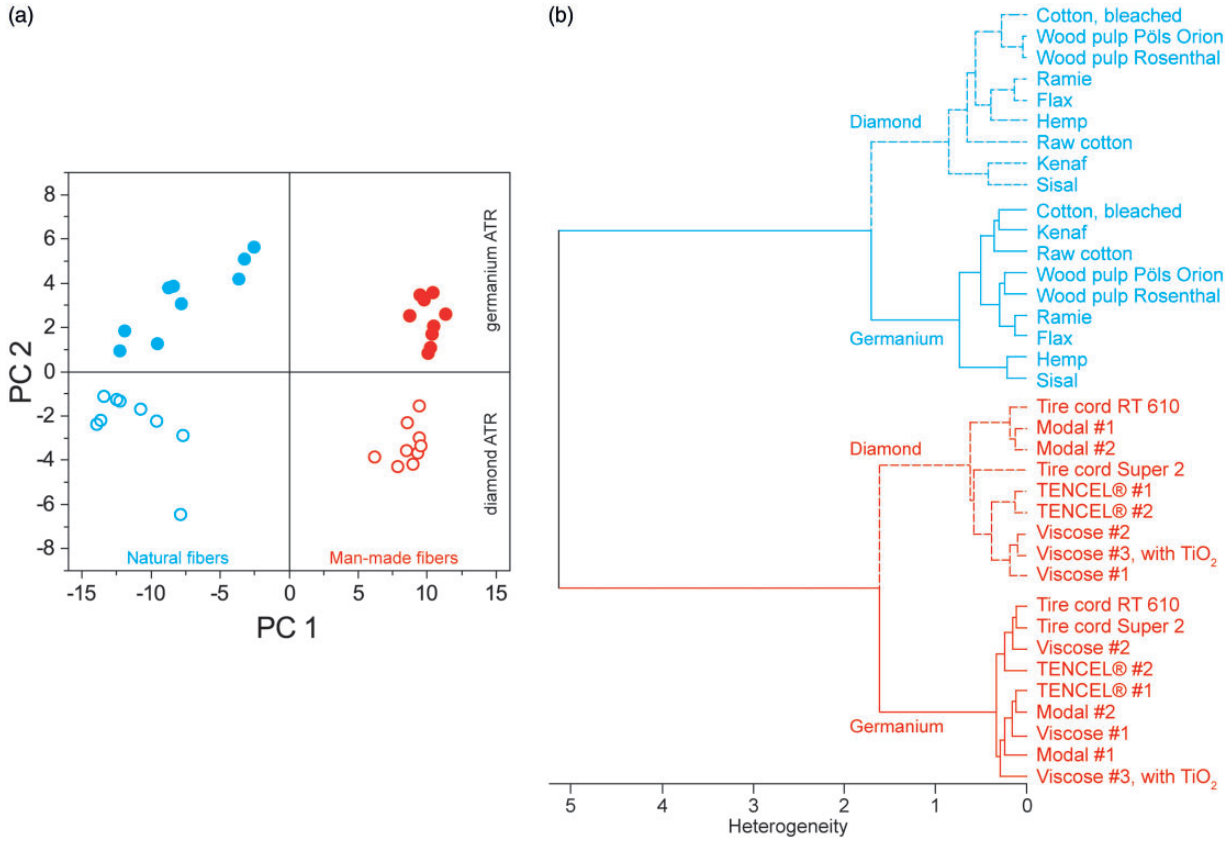

Figure 6. (a) Score plots of PC1 vs. PC2 obtained by PCA analysis of ATR spectra (germanium and diamond) of all fiber samples. (b) Dendrogram of all ATR spectra of man-made and natural cellulose fibers using the Ward's method and the Euclidean distance measure.

acquired while changing the humidity level. These measurements were performed with a natural fiber (raw cotton) and a man-made fiber (Tencel® #1) sample using the platinum ATR unit. Prior to humidity modulation (time < 0), spectra were taken at ambient conditions (temperature: 25.4 °C, relative humidity: ~45%). In order to induce drying of the fibers, the sample compartment of the instrument was closed and flushed with dry air (time = 0). After 120 min, the sample compartment was opened again and the fibers were exposed to ambient humidity, leading to rehydration of the fiber sample.

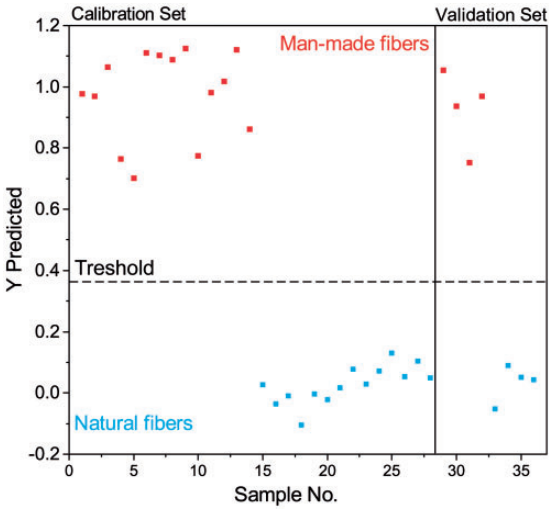

Figure 7. Score plot of the class prediction of samples included in the calibration (28 data points) and validation set (8 data points).

Figure 8 shows the effect of changing water content on the IR spectra of the two fiber samples. The overall behavior of the raw cotton and Tencel® #1 sample are comparable. The most significant impact is observed for the band with a maximum at 1640 cm^{-1}, attributed to the HOH bending band of absorbed water. Comparable behavior has been observed before for different kinds of plant fibers.[16] The temporal progression of the band area is shown in the inset of Figure 8. Upon flushing with dry air, the band intensity continually decreases until reaching a minimum value, and remains constant after about 100 minutes. After exposing the fibers again to the humidity of the ambient atmosphere, the band intensity increases back to approximately the initial value.

Further significant changes in the IR spectrum were found at the broad band located between 3600 and 3000 cm^{-1}. This spectral region is associated to formation of hydrogen bonds between water and hydroxyl groups of cellulose or hemicellulose. Decreasing intensity of this band at lower relative humidity content has been observed in earlier studies.[16,41]

As highlighted by the close-up view (see Figure 8, right), there are also intensity changes in the fingerprint region caused by modulation of the relative humidity content. Absorption bands in the spectral region ranging from 1150–800 cm^{-1} are associated with stretching vibrations of the C–O–C group of polysaccharide components within the studied fibers.[36] It has been argued that the altered nature of intramolecular bonding (as outlined above) leads to a modified stress transfer along the

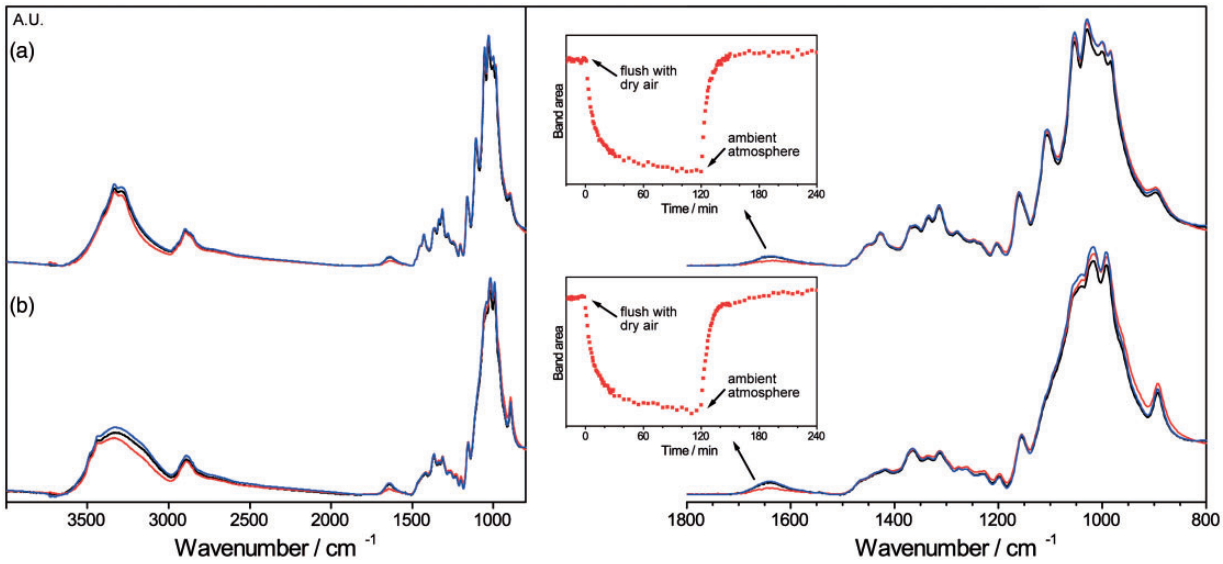

Figure 8. (left) ATR FT-IR absorbance spectra of (a) raw cotton and (b) Tencel® #1 fiber samples. (right) Close-up view of the spectral range 1800–800 cm^{-1}. Spectra are recorded at initial humid state (0 min, black), dried state (120 min, red), and re-humidified state (240 min, blue). Insets show the progression of the band area assigned to absorbed water (~1640 cm^{-1}) with changing humidity.

cellulose chain, which in turn affects the corresponding vibration energies of the carbohydrate backbone.[42]

Library search was performed for IR spectra of fiber samples taken in the initial humid state, dried state and re-humidified state. Both groups of fiber samples were correctly identified by the search routine for every spectrum. Regarding the cotton sample, the first three library hits for IR spectra of each state revealed the same three natural fibers regardless of the amount of absorbed water. Also for the Tencel® fiber sample, the first three findings showed man-made fiber samples in every case. Hit results were the same for initial humid and dry states; however, different findings were suggested for the re-humidified state. The employed spectral library did not provide any information about the humidity of the fiber.

Conclusion

This work presents a comprehensive analysis of natural and man-made fibers by FT-IR spectroscopy. For this purpose, three spectra acquisition techniques including ATR microscopy (IRE: germanium), transmission microscopy and ATR spectroscopy (IRE: diamond) have been evaluated. Representative bands in the fingerprint and OH stretching region could be identified and assigned to characteristic vibrations of natural and man-made fibers. Moreover, the influence of different levels of humidity on the IR spectra of fiber samples was investigated.

In order to establish a routine to discriminate between natural and man-made fibers, spectra library search, HCA, PCA, and PLS-DA were evaluated. Library search may be employed in case no reference fibers are easily available for comparison. Here, this approach was performed to evaluate its applicability for identification of the respective fiber types. To this end, results of the three IR acquisition methods were compared. Using transmission microscopy, only 60% of natural fiber spectra were correctly identified as natural fibers and 40% were wrongly identified as man-made fibers. It was also found that the library search provides better results when the library spectra have been recorded with the same acquisition method (transmission vs. ATR) as the sample spectra. Further, the type of search algorithm as well as data processing play a crucial role on the successful usage of library search. In an alternative approach, the potential of HCA was examined for discrimination between natural and man-made fibers. This method is applicable, if reference samples for both fiber types are available. Successful clustering into two classes was obtained for IR spectra obtained by ATR microscopy and ATR spectroscopy, using the optimized spectra processing and HCA parameters. Whereas a clear influence of the type of IRE on the recorded spectra could be observed, it appeared that the difference in the spectra due to the fiber type (natural vs. man-made) was more pronounced. In any case, for most reliable classification it is strongly recommended to use the same type of IRE for library and sample spectra. An appropriate means to distinguish between man-made and natural cellulosic fibers may be PLS-DA. However, also in this case it remains to be investigated how a partial degradation and weathering of the fibers of different classes in the environment affects correct classification.

Acknowledgments

We acknowledge Hans Lohninger from the Vienna University of Technology for discussions about the chemometric treatment of the obtained data set. Further, we thank Bruker GmbH, Germany for providing the employed spectral libraries for testing purposes.

Conflict of Interest

The authors report there are no conflicts of interest.

Funding

I.R.C.-S. gratefully acknowledges the financial support to Sectorial Operational Programme Human Resources Development 2007-2013 of the Ministry of European Funds through the Financial Agreement POSDRU/159/1.5/S/132395.

References

1. G. Liebezeit, E. Liebezeit. "Synthetic Particles as Contaminants in German Beers". Food Addit. Contam., Part A. 2014. 31(9): 1574–1578.
2. G. Liebezeit, E. Liebezeit. "Non-Pollen Particulates in Honey and Sugar". Food Addit. Contam., Part A. 2013. 30(12): 2136–2140.
3. D.W. Lachenmeier, J. Kocareva, D. Noack, T. Kuballa. "Microplastic Identification in German Beer – an Artefact of Laboratory Contamination?". Dtsch. Lebensm.-Rundsch. 2015. 111(10): 437–440.
4. L.C. Woodall, C. Gwinnett, M. Packer, R.C. Thompson, L.F. Robinson, G.L.J. Paterson. "Using a Forensic Science Approach to Minimize Environmental Contamination and to Identify Microfibres in Marine Sediments". Mar. Pollut. Bull. 2015. 95(1): 40–46.
5. M.A. Browne, P. Crump, S.J. Niven, E. Teuten, A. Tonkin, T. Galloway, R. Thompson. "Accumulation of Microplastic on Shorelines Worldwide: Sources and Sinks". Environ. Sci. Technol. 2011. 45(21): 9175–9179.
6. A.L. Lusher, M. McHugh, R.C. Thompson. "Occurrence of Microplastics in the Gastrointestinal Tract of Pelagic and Demersal Fish from the English Channel". Mar. Pollut. Bull. 2013. 67(1–2): 94–99.
7. L.C. Woodall, A. Sanchez-Vidal, M. Canals, G.L.J. Paterson, R. Coppock, V. Sleight, A. Calafat, A.D. Rogers, B.E. Narayanaswamy, R.C. Thompson. "The Deep Sea is a Major Sink for Microplastic Debris". R. Soc. Open Sci. 2014. 1(4): 140317.
8. Wikipedia. "Rayon". https://en.wikipedia.org/wiki/Rayon (accessed May 30 2016).
9. D. Ciechańska, E. Wesołowska, D. Wawro. "An Introduction to Cellulosic Fibres". In: S.J. Eichhorn, J.W.S. Hearle, M. Jaffe, T. Kikutani (eds) Handbook of Textile Fibre Structure. Cambridge, UK: Woodhead Publishing, 2009.
10. H. Sixta (ed.) Handbook of Pulp. Weinheim, Germany: Wiley-VCH, 2008.
11. O. Faruk, A.K. Bledzki, H.-P. Fink, M. Sain. "Progress Report on Natural Fiber Reinforced Composites". Macromol. Mater. Eng. 2014. 299(1): 9–26.
12. J. Ganster, H.P. Fink. "The Structure of Man-Made Cellulosic Fibres". In: S.J. Eichhorn, J.W.S. Hearle, M. Jaffe, T. Kikutani (eds) Handbook of Textile Fibre Structure. Cambridge, UK: Woodhead Publishing, 2009.

13. K. Bredereck, F. Hermanutz. "Man-Made Cellulosics". Rev. Prog. Color. Relat. Top. 2005. 35(1): 59–75.
14. P. Garside, P. Wyeth. "Identification of Cellulosic Fibres by FTIR Spectroscopy". Stud. Conserv. 2003. 48(4): 269–275.
15. M. Fan, D. Dai, B. Huang. "Fourier Transform Infrared Spectroscopy for Natural Fibres". In: S.M. Salih (ed.) Fourier Transform – Materials Analysis. China: InTech, 2012.
16. A. Celino, O. Goncalves, F. Jacquemin, S. Freour. "Qualitative and Quantitative Assessment of Water Sorption in Natural Fibres using ATR-FTIR Spectroscopy". Carbohydr. Polym. 2014. 101: 163–170.
17. C. Yan, B. Yang, Z.C. Yu. "Terahertz Time Domain Spectroscopy for the Identification of Two Cellulosic Fibers with Similar Chemical Composition". Anal. Lett. 2013. 46(6): 946–958.
18. A. Carrillo, X. Colom, J.J. Sunol, J. Saurina. "Structural FTIR Analysis and Thermal Characterisation of Lyocell and Viscose-Type Fibres". Eur. Polym. J. 2004. 40(9): 2229–2234.
19. F. Carrillo, X. Colom, J. Valldeperas, D. Evans, M. Huson, J. Church. "Structural Characterization and Properties of Lyocell Fibers after Fibrillation and Enzymatic Defibrillation Finishing Treatments". Text. Res. J. 2003. 73(11): 1024–1030.
20. X. Colom, F. Carrillo. "Crystallinity Changes in Lyocell and Viscose-Type Fibres by Caustic Treatment". Eur. Polym. J. 2002. 38(11): 2225–2230.
21. D. Klemm, B. Heublein, H.-P. Fink, A. Bohn. "Cellulose: Fascinating Biopolymer and Sustainable Raw Material". Angew. Chem. Int. Ed. 2005. 44(22): 3358–3393.
22. P.H. Hermans, A. Weidinger. "X-Ray Studies on the Crystallinity of Cellulose". J. Polym. Sci. 1949. 4(2): 135–144.
23. P.T. Larsson, K. Wickholm, T. Iversen. "A CP/MAS C-13 NMR Investigation of Molecular Ordering in Celluloses". Carbohydr. Res. 1997. 302(1–2): 19–25.
24. G. Zuckerstätter, N. Terinte, H. Sixta, K.C. Schuster. "Novel Insight into Cellulose Supramolecular Structure through ^{13}C CP-MAS NMR Spectroscopy and Paramagnetic Relaxation Enhancement". Carbohydr. Polym. 2013. 93(1): 122–128.
25. T. Baldinger, J. Moosbauer, H. Sixta. "Supermolecular Structure of Cellulosic Materials by Fourier Transform Infrared Spectroscopy (FT-IR) Calibrated by WAXS and ^{13}C NMR". Lenzinger Ber. 2000. 79: 15–17.
26. L. Kaufman, P.J. Rousseeuw. Finding Groups in Data. Hoboken, NJ: John Wiley & Sons, Inc., 2005.
27. S. Navea, R. Tauler, E. Goormaghtigh, A. de Juan. "Chemometric Tools for Classification and Elucidation of Protein Secondary Structure from Infrared and Circular Dichroism Spectroscopic Measurements". Proteins. 2006. 63(3): 527–541.
28. N. Cebi, M.Z. Durak, O.S. Toker, O. Sagdic, M. Arici. "An Evaluation of Fourier Transforms Infrared Spectroscopy Method for the Classification and Discrimination of Bovine, Porcine and Fish Gelatins". Food Chem. 2016. 190: 1109–1115.
29. A. Domenighini, M. Giordano. "Fourier Transform Infrared Spectroscopy of Microalgae as a Novel Tool for Biodiversity Studies, Species Identification, and the Assessment of Water Quality". J. Phycol. 2009. 45(2): 522–531.
30. M. Barker, W. Rayens. "Partial Least Squares for Discrimination". J. Chemom. 2003. 17(3): 166–173.
31. P.R. Griffiths, J.A. de Haseth. Fourier Transform Infrared Spectrometry. Hoboken, NJ: John Wiley & Sons, Inc., 2006.
32. Lohninger, H.H. "Datalab 3.5, a Programme for Statistical Analysis". 2000. http://datalab.epina.at/ (accessed May 30 2016).
33. G. Ramer, B. Lendl. "Attenuated Total Reflection Fourier Transform Infrared Spectroscopy". In: Encyclopedia of Analytical Chemistry. Hoboken, NJ: John Wiley & Sons, Inc., 2013.
34. A. Stamboulis, C.A. Baillie, T. Peijs. "Effects of Environmental Conditions on Mechanical and Physical Properties of Flax Fibers". Composites, Part A. 2001. 32(8): 1105–1115.
35. M.P. Ansell, L.Y. Mwaikambo. "The Structure of Cotton and Other Plant Fibres". In: S.J. Eichhorn, J.W.S. Hearle, M. Jaffe, T. Kikutani (eds) Handbook of Textile Fibre Structure. Cambridge, UK: Woodhead Publishing, 2009.
36. A. Celino, S. Freour, F. Jacquemin, P. Casari. "Characterization and Modeling of the Moisture Diffusion Behavior of Natural Fibers". J. Appl. Polym. Sci. 2013. 130(1): 297–306.
37. L.Y. Mwaikambo, M.P. Ansell. "Chemical Modification of Hemp, Sisal, Jute, and Kapok Fibers by Alkalization". J. Appl. Polym. Sci. 2002. 84(12): 2222–2234.
38. V. Titok, V. Leontiev, S. Yurenkova, T. Nikitinskaya, T. Barannikova, L. Khotyleva. "Infrared Spectroscopy of Fiber Flax". J. Nat. Fibers. 2010. 7(1): 61–69.
39. M.L. Nelson, R.T. O'Connor. "Relation of Certain Infrared Bands to Cellulose Crystallinity and Crystal Latticed Type. Part I. Spectra of Lattice Types I, II, III and of Amorphous Cellulose". J. Appl. Polym. Sci. 1964. 8(3): 1311–1324.
40. A. Célino, S. Freour, F. Jacquemin, P. Casari. "The Hygroscopic Behavior of Plant Fibres: A Review". Front. Chem. 2014. 1: 43.
41. K. Hofstetter, B. Hinterstoisser, L. Salmen. "Moisture Uptake in Native Cellulose – the Roles of Different Hydrogen Bonds: A Dynamic FT-IR Study using Deuterium Exchange". Cellulose. 2006. 13(2): 131–145.
42. A.-M. Olsson, L. Salmén. "The Association of Water to Cellulose and Hemicellulose in Paper Examined by FTIR Spectroscopy". Carbohydr. Res. 2004. 339(4): 813–818.